Superfluid Fermi Gas in Optical Lattices: Self-Trapping, Stable, Moving Solitons and Breathers

Ju-Kui Xue* and Ai-Xia Zhang

Physics and Electronics Engineering College, Northwest Normal University, Lanzhou 730070, People's Republic of China

(Received 10 March 2008; published 28 October 2008)

We predict the existence of self-trapping, stable, moving solitons and breathers of Fermi wave packets along the Bose-Einstein condensation (BEC)-BCS crossover in one dimension (1D), 2D, and 3D optical lattices. The dynamical phase diagrams for self-trapping, solitons, and breathers of the Fermi matter waves along the BEC-BCS crossover are presented analytically and verified numerically by directly solving a discrete nonlinear Schrödinger equation. We find that the phase diagrams vary greatly along the BEC-BCS crossover; the dynamics of Fermi wave packet are different from that of Bose wave packet.

DOI: 10.1103/PhysRevLett.101.180401 PACS numbers: 03.75.Lm, 03.75.Kk, 03.75.Ss

Recently, superfluid Fermi gases in optical lattices have attracted much attention both experimentally and theoretically. The superfluidity of ultracold fermions in optical lattices has been established [1]. In such a superfluid system, the physical parameters, e.g., lattice parameters, interaction strength, etc., can be manipulated by using a modern experimental technique like Feshbach resonance. Taking advantage of this, people have given many theoretical efforts on the crossover from Bose-Einstein condensation (BEC) to Bardeen-Cooper-Schrieffer (BCS) state in optical lattices, such as Bloch oscillations [2], superfluid-insulator transitions [3,4], and the collective excitations [5,6]. The intrinsically localized excitations, i.e., gap solitons (shape-preserving objects supported by the balance between the repulsive nonlinearity and negative effective mass induced by lattices potential [7,8]), in Fermi gases trapped in 1D optical lattices are also predicted [7]. To our knowledge, however, there are no systematically analyses of the dynamics of Fermi gases loaded into 3D optical lattices. Especially, self-trapping (characterized by a diverging effective mass, and the wave packet remaining localized around few sites), an intriguing phenomenon has been observed in Bose systems [8–13] but was not studied in Fermi systems. Thus, there remain some important problems, e.g., how the dynamical properties behave in a Fermi system.

In this Letter, we address this issue both analytically and numerically focusing on the dynamics of Fermi gases in deep 3D optical lattices, within the tight-binding approximation. Based on a discrete, nonlinear Schrödinger equation, the phase diagram for self-trapping, soliton (gap type), breather (characterized by internal oscillations and created in a gap soliton) [8], diffusion of the Fermi matter waves in 3D optical lattices is obtained analytically. Our results show many new and interesting consequences. (i) The self-trapped state of Fermi wave packets can exist in 1D, 2D, and 3D optical lattices along the BEC-BCS crossover. (ii) The stable moving soliton and breather solutions of Fermi wave packet along the BEC-BCS crossover in both 1D and 2D systems can exist, while for the 3D case, the stable moving soliton and breather solutions can exist only in the BCS side. This point is different from the Bose system (in the Bose system, the stable moving soliton and breather solutions can exist only in 1D lattices [11]). (iii) The critical conditions for the occurrence of self-trapping, soliton, and breather solutions change dramatically when the system transitions from the BEC side to the BCS side. The self-trapped, soliton, and breather states take place in the BCS side always easier than those in the BEC side. Moreover, the critical conditions for the occurrence of self-trapping, soliton, and breather solutions in both BEC and BCS sides increase sharply with lattice dimension.

Consider an interacting two equally populated spin components superfluid Fermi gas of N atoms trapped in 3D optical lattices. For large enough N, we assume that the Cooper pair size is smaller than the lattice spacing and the system behaves hydrodynamically from the molecular BEC side to BCS side [1,2]. Under these assumptions, the dynamics of this 3D Fermi system at $T = 0$ satisfies the nonlinear Schrödinger equation [14–19]

$$i\hbar \frac{\partial \Psi}{\partial t} = \left[-\frac{\hbar^2}{2M}\nabla^2 + V_{\mathrm{opt}}(\vec{r}) + \mu(n) \right]\Psi \qquad (1)$$

where Ψ is the superfluid order parameter, $V_{\mathrm{opt}}(\vec{r}) = sE_R[\cos(2\pi x/d) + \cos(2\pi y/d) + \cos(2\pi z/d)]$ is the external optical potential created by three orthogonal pairs of counter-propagating laser beams, with the parameters s the strength of the optical lattices and $E_R = \hbar^2\pi^2/2Md^2$ the recoil energy of the lattices; d is the lattice period and M is the mass of one atom (in the BEC side, the mass of the Cooper pair should be $2M$ and the number of the pairs should be $N/2$). We assume the power-law form of the equation of state as $\mu(n) = C|\Psi|^{2\gamma}$, which is being used successfully to study the Fermi superfluid along the crossover [15–19]. Here, C is a constant depending on the atoms' interaction strength [18] and γ is a function of an interaction parameter $\eta = 1/k_F a$, where k_F is the Fermi wave vector and a is the scattering length between Fermi atoms of different components (in the BEC side, the effective scattering length between the paired molecules should be $0.6a$). At $T = 0$, the energy per particle of a dilute

Fermi system is $\epsilon = (3/5)E_F\epsilon(\eta)$, where $E_F = \hbar^2 k_F^2/2M$ is the free particle Fermi energy and $\epsilon(\eta)$ is a function of the interaction parameter η. Recently, a simple analytical expression for $\epsilon(\eta)$ with only one free parameter along the BEC-BCS crossover was given [20]. Here, the expression for $\epsilon(\eta)$ given in Ref. [18] is applied. Then the chemical potential μ and the effective adiabatic index γ can be obtained [18].

When the lattice depth is sufficiently high, the Fermi energy is small compared to the interband gap, and the energy of the system should be confined within the lowest band. So one can work in the tight-binding limit [8,11]. Under the tight-binding approximation, the order parameter can be written as $\Psi(\vec{r}, t) = \sqrt{N}\sum_{n,m,k}\psi_{n,m,k}(t)\phi(\vec{r} - \vec{r}_{n,m,k})$, where $\psi_{n,m,k}(t)$ is the (n, m, k)th amplitude and $\phi(\vec{r} - \vec{r}_{n,m,k})$ is the Wannier function of the lowest band localized in the site (n, m, k), with the normalization $\int d\vec{r}\phi^2_{n,m,k} = 1$. Inserting this nonlinear tight-binding approximation into Eq. (1) and integrating out the spatial degrees of freedom, we find the reduced dimensionless 3D discrete nonlinear Schrödinger equation $\dot{\psi}_{n,m,k} = \partial H/\partial(i\psi^*_{n,m,k})$, where H is the Hamiltonian function

$$H = \sum_{n,m,k}\Big[-\frac{1}{2}(\psi_{n,m,k}\psi^*_{n+1,m,k} + \psi^*_{n,m,k}\psi_{n+1,m,k} + \psi_{n,m,k}\psi^*_{n,m+1,k} + \psi^*_{n,m,k}\psi_{n,m+1,k} + \psi_{n,m,k}\psi^*_{n,m,k+1} + \psi^*_{n,m,k}\psi_{n,m,k+1}) + \varepsilon|\psi_{n,m,k}|^2 + \frac{\Lambda}{1+\gamma}|\psi_{n,m,k}|^{2(\gamma+1)}\Big] \quad (2)$$

with $\sum_{n,m,k}|\psi_{n,m,k}|^2 = 1$. The terms in parentheses are kinetic energies of n, m, k components, and the variables have been rescaled as $t \to [\hbar/(2J)]t$, $\varepsilon \to \varepsilon/2J$. Here, $\Lambda = U/2J$, J is the tunneling rate between the adjacent sites, U is the effective on-site interaction, and ε is the on-site energies. Loading a Fermi gas into 1D or 2D optical lattices, and confining in the transverse direction(s) by a tight cigar-shaped or pancake-shaped trap, Eq. (2) can be extended to 1D (the kinetic terms of m and k components are absent) or 2D (the kinetic term of the k component is absent) case with modified nonlinear interaction parameter Λ.

We consider the evolution of a Gaussian ansatz, which we parametrize as $\psi_{n,m,k}(t) = \frac{2^{(D/4)}}{R^{(D/2)}\pi^{(D/4)}} \times \exp\{-\frac{(n-\xi)^2+(m-\xi)^2+(k-\xi)^2}{R^2} + ip[(n-\xi)+(m-\xi)+(k-\xi)] + i\frac{\delta}{2}[(n-\xi)^2+(m-\xi)^2+(k-\xi)^2]\}$, where $\xi(t)$ and $R(t)$ are the center and the width of the wave packet, $p(t)$ and $\delta(t)$ are their associated momenta, and $D = 1, 2, 3$ refer to the dimension of the optical lattices. In our 3D Fermi system, we have defined $\xi_x = \xi_y = \xi_z = \xi$, $R_x = R_y = R_z = R$, $p_x = p_y = p_z = p$, $\delta_x = \delta_y = \delta_z = \delta$. It is important to note that, for the 1D (2D) case, the m and k components (the k component) of the Gaussian ansatz should be dropped. The wave packet dynamical evolution can be obtained by a variational principle from the Lagrangian $L = \sum_{n,m,k} i(\dot{\psi}_{n,m,k}\psi^*_{n,m,k} - \psi_{n,m,k}\dot{\psi}^*_{n,m,k}) - H$, with the equations of motion for the variational parameters $q_i(t) = \xi, R, p, \delta$ given by $\frac{d}{dt}\frac{\partial L}{\partial \dot{q}_i} = \frac{\partial L}{\partial q_i}$. For an untilted trap, the momentum p remains a constant p_0, and the equations of motion of collective variables $\xi(t)$, $R(t)$, $\delta(t)$ in the 1D, 2D, and 3D cases are given by

$$\dot{\delta} = \cos p_0\left(\frac{2}{R^4} - \frac{\delta^2}{2}\right)e^{-\sigma} + \frac{2\Lambda\gamma}{(1+\gamma)^{(2+D)/2}R^{D\gamma+2}}\left(\frac{2}{\pi}\right)^{(D\gamma/2)},$$
$$\dot{R} = \frac{R}{2}\delta e^{-\sigma}\cos p_0, \qquad \dot{\xi} = \frac{1}{2}e^{-\sigma}\sin p_0 \quad (3)$$

where $\sigma = \frac{1}{2R^2} + \frac{R^2\delta^2}{8}$. Initially, we set $\xi_0 = 0$ and $\delta_0 = 0$. In this case, the effective Hamiltonian becomes

$$H = -D(\cos p_0)e^{-\sigma} + \frac{\Lambda}{(1+\gamma)^{(D+2)/2}}\frac{1}{R^{D\gamma}}\left(\frac{2}{\pi}\right)^{(D\gamma/2)}. \quad (4)$$

Clearly, the dynamical properties of the system are influenced by the atoms' interaction parameter γ, the dimension of optical lattices D, and the initial quasimomentum p_0. We should note that, when $\cos p_0 < 0$, the effective mass $\frac{1}{m^*} \equiv \frac{\partial^2 H}{\partial p_0^2} = De^{-\sigma}\cos p_0$ is negative and the system can exist in a soliton solution [7,8]. So two cases with $\cos p_0 > 0$ and $\cos p_0 < 0$ will be discussed, respectively.

For $\cos p_0 < 0$, we give the results as follows:

Self-trapping.—When the diffusion occurs, $R \to \infty$, $H \to -D\cos p_0$, thus in this case the self-trapping condition should be $H_0 > D|\cos p_0|$, this results in

$$\Lambda > \Lambda_c = D(1+\gamma)^{(D+2)/2}\left(\sqrt{\frac{\pi}{2}}R_0\right)^{D\gamma}|\cos p_0| \times\left(1 - e^{-(1/2R_0^2)}\right). \quad (5)$$

This condition gives the self-trapped state, while for $\Lambda < \Lambda_c$ the diffusion should occur. When the self-trapping occurs, $R \to R_{\min} < R_0$, $\delta \to \infty$, $\dot{\xi} \to 0$, and $H \to \frac{\Lambda}{(1+\gamma)^{(D+2)/2}}\frac{1}{R_{\min}^{D\gamma}}(\frac{2}{\pi})^{D\gamma/2}$. From $H_0 = H$, one can get $R_{\min} = R_0[(\Lambda/\Lambda')/(1+\Lambda/\Lambda')]^{(1/D\gamma)}$, where $\Lambda' = D(1+\gamma)^{(D+2)/2}(\pi/2)^{D\gamma/2}R_0^{D\gamma}|\cos p_0|e^{-(1/2R_0^2)}$.

Soliton.—The soliton solution of the system corresponds to the fixed points $\dot{R} = 0$, $\dot{\delta} = 0$, and $\dot{\xi} =$ constant. From Eq. (3), the fixed point (δ_0, R_0) satisfies $\delta_0 = 0$ and

$$\Lambda_{\rm sol} = \frac{(1+\gamma)^{(D+2)/2}}{\gamma}\left(\frac{\pi}{2}\right)^{(D\gamma/2)}R_0^{D\gamma-2}|\cos p_0|e^{-(1/2R_0^2)}. \quad (6)$$

We now discuss the stability of this soliton state. Defining $\delta = \delta_0 + \delta'$, $R = R_0 + R'$, and linearizing Eq. (3) at the soliton state, we have

$$\begin{pmatrix}\dot{\delta}'\\ \dot{R}'\end{pmatrix} = A\begin{pmatrix}0 & 4(2 - D\gamma - 1/R_0^2)\\ -R_0^6 & 0\end{pmatrix}\begin{pmatrix}\delta'\\ R'\end{pmatrix} \quad (7)$$

where $A = \frac{\Lambda}{4}\frac{2\gamma}{(1+\gamma)^{(2+D)/2}}(\frac{2}{\pi})^{(D\gamma/2)}\frac{1}{R_0^{D\gamma+3}}$. The eigenvalues of the coefficient matrix of Eq. (7) satisfy $\lambda^2 = 4R_0^6(D\gamma + 1/R_0^2 - 2)$. For $R_0 > 1$, if the condition

$$D\gamma < 2 \tag{8}$$

is satisfied, the soliton state corresponds to a center point; in this case the soliton state is stable and a breather state can also exist. Clearly, the stability of the soliton state greatly depends on the dimension of the optical lattices D and γ. For a Bose system (i.e., a perfect BEC system), $\gamma \equiv 1$, Eq. (8) indicates that the soliton and breather states can exist only in the $D = 1$ case [11]. While for a Fermi system, the situation is quite different. In the BEC side, $\frac{2}{3} < \gamma < 1$, the condition (8) can be satisfied when $D \leq 2$. That is, stable soliton and breather states can stand not only in 1D case but in 2D case. More interestingly, in the BCS side, $\gamma \leq \frac{2}{3}$, we have $D \leq 3$, stable soliton state and breather state can appear in 1D, 2D, even 3D Fermi systems. These are the key results of the Letter and will be confirmed by direct numerical results.

$\Lambda = \Lambda_{\rm sol}$ corresponds to a soliton solution, R remains the initial value R_0, and $\dot{\xi} =$ constant. For $\Lambda_c < \Lambda < \Lambda_{\rm sol}$, R oscillates between the initial value R_0 and a value $R_{\rm osc}^{\rm max} > R_0$; we have a breather solution. The breather region extends until the value $\Lambda_{\rm breath}$, for $\Lambda_{\rm sol} < \Lambda < \Lambda_{\rm breath}$, R oscillates between the initial value R_0 and a value $R_{\rm osc}^{\rm min} < R_0$. The determination of $\Lambda_{\rm breath}$ is as follows. When $\Lambda_{\rm sol} < \Lambda < \Lambda_{\rm breath}$, we find $R \to R_{\rm osc}^{\rm min} < R_0$ and $\delta = 0$, then $H \to D|\cos p_0|e^{-(1/2R_{\rm min}^2)} + \frac{\Lambda}{(1+\gamma)^{\frac{D+2}{2}}}\frac{1}{R_{\rm min}^{D\gamma}} \times (\frac{2}{\pi})^{(D\gamma/2)}$. By using the energy conservation $H_0 = H$, we get $\Lambda/\Lambda_{\rm sol} = D\gamma R_0^2 x^{D\gamma}(e^{(x^2-1)/2R_0^2x^2} - 1)/(x^{D\gamma} - 1)$, where $R_{\rm min} = xR_0$, $x < 1$. It is clear that, as expected, when $x \to 1$, $\Lambda \to \Lambda_{\rm sol}$. Because $R_0 > 1$, the maximum value of the ratio of $\Lambda/\Lambda_{\rm sol}$ gives $\Lambda_{\rm breath}/\Lambda_{\rm sol}$

$$\Lambda_{\rm breath} = \Lambda_{\rm sol}\max_{0<x<1}\left\{\frac{D\gamma R_0^2 x^{D\gamma}}{1 - x^{D\gamma}}(1 - e^{(x^2-1)/2R_0^2x^2})\right\}. \tag{9}$$

The critical values for the occurrence of self-trapping Λ_c, soliton $\Lambda_{\rm sol}$, and breather $\Lambda_{\rm breath}$ along the BEC-BCS crossover are shown in Figs. 1(a)–1(i) for the $\cos p_0 < 0$ case. The first, second, and third panels correspond to 1D, 2D, and 3D Fermi systems, respectively. The critical values Λ_c, $\Lambda_{\rm sol}$, $\Lambda_{\rm breath}$ in both BEC and BCS sides increase sharply as D increases. For an initial Fermi wave packet, the higher the dimension is, the larger the critical values needed to observe the self-trapped, soliton, and breather states. Moreover, compared to the results in the BEC side, the critical values Λ_c, $\Lambda_{\rm sol}$, $\Lambda_{\rm breath}$ in the BCS side are always small. The self-trapped, soliton, and breather states take place in BCS superfluid always easier than those in BEC superfluid.

For $\cos p_0 > 0$, there exist only two nonlinear physical phenomena.

Self-trapping.—For $t \to \infty$, $R \to R_{\rm max}$, $\delta \to \infty$, and $\dot{\xi} \to 0$, $H \to \frac{\Lambda}{(1+\gamma)^{(D+2)/2}}\frac{1}{R_{\rm max}^{D\gamma}}(\frac{2}{\pi})^{D\gamma/2} > 0$.

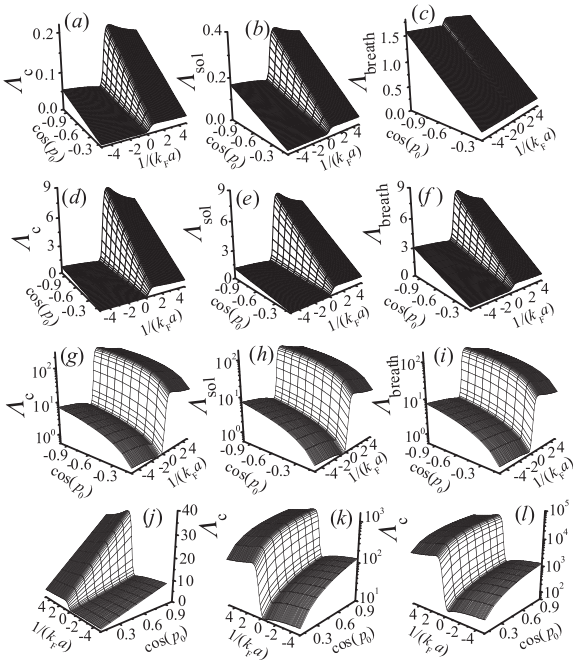

FIG. 1. The critical values, from left to right, Λ_c, $\Lambda_{\rm sol}$, $\Lambda_{\rm breath}$ along the BEC($1/k_Fa > 0$) − BCS($1/k_Fa < 0$) crossover for $\cos p_0 < 0$ (the first panel for 1D, the second panel for 2D, the third panel for 3D) and the critical values Λ_c along the BEC-BCS crossover for $\cos p_0 > 0$ (the fourth panel, from left to right, for 1D, 2D, and 3D cases), $R_0 = 10$.

Diffusion.—In this case, for $t \to \infty$, $R \to \infty$, $\delta \to 0$, and $\dot{\xi} \to \frac{1}{2}\sin p_0$, $H \to -D\cos p_0 < 0$. So the condition $-D\cos p_0 \leq H_0 \leq 0$ corresponds to the diffusive region of the system. The critical condition between self-trapping and diffusion is given by $H_0 = 0$; one can get

$$\Lambda_c = D(1+\gamma)^{(D+2)/2}(\pi/2)^{D\gamma/2}R_0^{D\gamma}e^{-(1/2R_0^2)}\cos p_0. \tag{10}$$

The self-trapping phenomenon occurs at $\Lambda > \Lambda_c$, and the diffusion occurs at $\Lambda < \Lambda_c$. Taking $H = H_0$, one obtains $R_{\rm max} = R_0[(\Lambda/\Lambda_c)/(\Lambda/\Lambda_c - 1)]^{1/D\gamma}$. The ratio of $R_{\rm max}/R_0$ depends on D and γ.

The critical values Λ_c along the BEC-BCS crossover given by Eq. (10) for $\cos p_0 > 0$ are shown in Fig. 1(j)–1(l) for 1D, 2D, and 3D Fermi systems, respectively. Clearly,

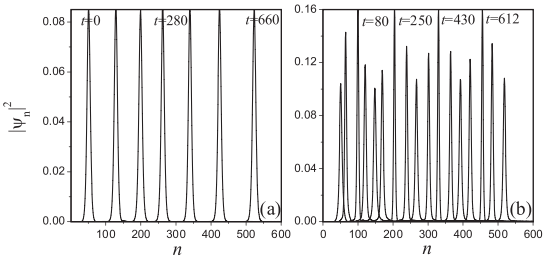

FIG. 2. The time evolution of the soliton state with $\Lambda = \Lambda_{\rm sol} = 0.1225$ (a) and the breather state with $\Lambda = 0.25 < \Lambda_{\rm breath} = 1.1$ (b) of a 1D wave packet, $R_0 = 10$, $p_0 = 3\pi/4$, $\gamma = 2/3$.

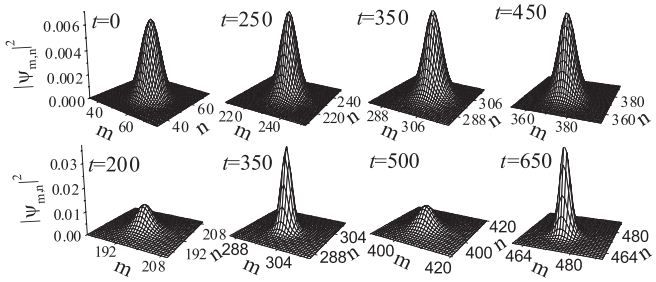

FIG. 3. The time evolution of the two-dimensional soliton state with $\Lambda = \Lambda_{\rm sol} = 0.85$ (the first panel) and breather state with $\Lambda = 1.25 < \Lambda_{\rm breath} \simeq 2.25$ (the second panel), $R_0 = 10$, $p_0 = 3\pi/4$, $\gamma = 2/3$.

the critical conditions for the occurrence of self-trapping in this case have similar properties as in the $\cos p_0 < 0$ case: D and γ have a strong effect on the critical conditions. We also can find that the critical values for $\cos p_0 > 0$ are larger than for $\cos p_0 < 0$.

The direct numerical solutions of Eq. (2) confirm our theoretical predictions. Here we only present the numerical results for BCS superfluid. Figure 2 shows the stable moving soliton solution (right) and breather solution (left) of a 1D Fermi wave packet in the BCS superfluid ($\gamma = 2/3$). In Fig. 3, the stable moving 2D soliton for $\Lambda = \Lambda_{\rm sol}$ (the first panel) and breather for $\Lambda < \Lambda_{\rm breath}$ (the second panel) are presented ($\gamma = 2/3$). Also, Fig. 4 shows the results for the evolution dynamics of a 3D Fermi wave packet ($\gamma = 0.6$). It is clear, stable moving 3D soliton (the first panel) and 3D breather (the second panel) states can exist in a 3D Fermi superfluid. The above numerical results support our analytical predications.

In summary, we analytically and numerically investigate the dynamics of a Fermi gas loaded into deep optical lattices. Self-trapping, stable moving soliton, and breather solutions of Fermi wave packet along the BEC-BCS crossover in 1D, 2D, and 3D systems are obtained. In addition, we find that the self-trapped, soliton, and breather states take place in the BCS side always easier than those in the BEC side. We hope that our studies will stimulate experiments in that direction.

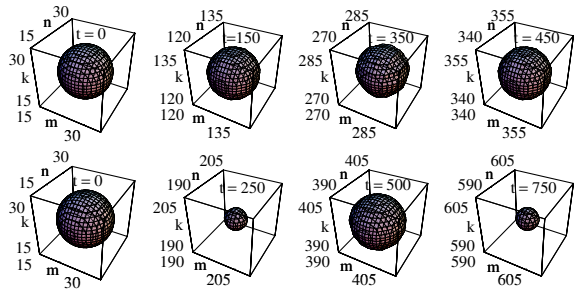

FIG. 4 (color online). The constant density surface of a 3D wave packet: The time evolution of the 3D soliton state with $\Lambda = \Lambda_{\rm sol} = 3.52$ (the first panel) and breather state with $\Lambda = 4 < \Lambda_{\rm breath} \simeq 4.4$ (the second panel), $R_0 = 10$, $p_0 = 3\pi/4$, $\gamma = 0.6$.

This work is supported by the National Natural Science Foundation of China (No. 10774120), by the Natural Science Foundation of Gansu province (No. 3ZS051-A25-013), and by NWNU-KJCXGC-03-17.

*Corresponding author: xuejk@nwnu.edu.cn

[1] J. K. Chin, D. E. Miller, Y. Liu, C. Stan, W. Setiawan, C. Sanner, K. Xu, and W. Ketterle, Nature (London) **443**, 961 (2006).
[2] M. Rodríguez and P. Törmä, Phys. Rev. A **69**, 041602 (2004); S. K. Adhikari, Eur. Phys. J. D **47**, 413 (2008).
[3] Hui Zhai and Tin-Lun Ho, Phys. Rev. Lett. **99**, 100402 (2007).
[4] Eun Gook Moon, Predrag Nikolić, and Subir Sachdev, Phys. Rev. Lett. **99**, 230403 (2007).
[5] L. P. Pitaevskii, S. Stringari, and G. Orso, Phys. Rev. A **71**, 053602 (2005).
[6] T. Koponen, J.-P. Martikainen, J. Kinnunen, and P. Törmä, Phys. Rev. A **73**, 033620 (2006).
[7] S. K. Adhikari and B. A. Malomed, Europhys. Lett. **79**, 50003 (2007); Phys. Rev. A **76**, 043626 (2007).
[8] A. Trombettoni and A. Smerzi, Phys. Rev. Lett. **86**, 2353 (2001); A. Smerzi and A. Trombettoni, Phys. Rev. A **68**, 023613 (2003); C. Menotti, A. Smerzi, and A. Trombettoni, New J. Phys. **5**, 112 (2003).
[9] T. Anker, M. Albiez, R. Gati, S. Hunsmann, B. Eiermann, A. Trombettoni, and M. K. Oberthaler, Phys. Rev. Lett. **94**, 020403 (2005).
[10] T. J. Alexander, E. A. Ostrovskaya, and Y. S. Kivshar, Phys. Rev. Lett. **96**, 040401 (2006); B. J. Dabrowska-Wuster, E. A. Ostrovskaya, T. J. Alexander, and Y. S. Kivshar, Phys. Rev. A **75**, 023617 (2007).
[11] Ju-Kui Xue, Ai-Xia Zhang, and Jie Liu, Phys. Rev. A **77**, 013602 (2008).
[12] BingbingWang, Panming Fu, Jie Liu, and BiaoWu, Phys. Rev. A **74**, 063610 (2006).
[13] P. G. Keverekidis, B. A. Malomed, D. J. Frantzeskakis, and R. Carretero-González, Phys. Rev. Lett. **93**, 080403 (2004).
[14] Y. E. Kim and A. L. Zubarev, Phys. Rev. A **70**, 033612 (2004).
[15] H. Hu, A. Minguzzi, X.-J. Liu, and M. P. Tosi, Phys. Rev. Lett. **93**, 190403 (2004).
[16] H. Heiselberg, Phys. Rev. Lett. **93**, 040402 (2004).
[17] A. Bulgac and G. F. Bertsch, Phys. Rev. Lett. **94**, 070401 (2005).
[18] N. Manini and L. Salasnich, Phys. Rev. A **71**, 033625 (2005).
[19] G. E. Astrakharchik, R. Combescot, X. Leyronas, and S. Stringari, Phys. Rev. Lett. **95**, 030404 (2005); G. E. Astrakharchik, J. Boronat, J. Casulleras, and S. Giorgini, Phys. Rev. Lett. **93**, 200404 (2004).
[20] S. K. Adhikari, Phys. Rev. A **77**, 045602 (2008).